Electronic Phase Separation in Manganite/Insulator Interfaces.

Luis Brey
Instituto de Ciencia de Materiales de Madrid (CSIC), Cantoblanco, 28049 Madrid, Spain.

By using a realist microscopic model, we study the electric and magnetic properties of the interface between a half metallic manganite and an insulator. We find that the lack of carriers at the interface debilitates the double exchange mechanism, weakening the ferromagnetic coupling between the Mn ions. In this situation the ferromagnetic order of the Mn spins near the interface is unstable against antiferromagnetic CE correlations, and a separation between ferromagnetic/metallic and antiferromagnetic/insulator phases at the interfaces can occur. We obtain that the insertion of extra layers of undoped manganite at the interface introduces extra carriers which reinforce the double exchange mechanism and suppress antiferromagnetic instabilities.

PACS numbers: 75.47.Gk,75.10.-b. 75.30Kz, 75.50.Ee.

I. INTRODUCTION

Half metallic ferromagnets are materials in which the electronic carriers at the Fermi energy have all the same spin direction. They are very promising materials for spintronics, since they can be used as spin polarized current injector and/or detector in magnetoelectronic devices.

For example, in a magnetic tunneling junction device the relative orientation of the magnetization of the two ferromagnetic electrodes affects dramatically the electron transport across the tunneling barrier connecting them[1, 2]. In these devices the tunneling magnetoresistance, TMR= $(R_{AP} - R_P)/R_{AP}$, where R_{AP} and R_P are respectively the resistances for antiparallel and parallel orientations, is directly related to the spin polarization of the electrodes by Jullière formula[3, 4] in such a way that as larger is the spin polarization of the electrodes, larger is the TMR. Independently of the details of the barrier,the TMR gets its maximum value when using half metallic electrodes[5]. Large values of TMR are desirable for optimal use of magnetic tunneling junctions in technological applications, and therefore the search for half metallic materials is one of the more active research area in solid state science[6].

Although several materials have been proposed to exhibit half-metallic conductivity, only in a small number of them this property has been experimentally confirmed. Some of the most studied half metallic materials are perovskites of manganese of formula $(R_{1-x}D_x)MnO_3$, where R denotes rare earth ions (R=La, Pr,...) and D is a divalent alkaline ion (D=Ca,Sr,...). These compounds are called generically manganites. In these oxides x coincides with the concentration of holes moving in the e_g orbital bands of the Mn ions that ideally form a cubic structure. For perovskites of the form $La_{1/3}D_{2/3}Mn\ O_3$, spin polarized photoemission experiments[7] and low temperature magnetoresistance measurements[8, 9] indicate an almost complete spin polarization of the carriers and the half metallicity character of these oxides.

The experimental evidence of the large spin polarization of manganites, particularly $La_{2/3}Ca_{1/3}MnO_3$ and $La_{2/3}Sr_{1/3}MnO_3$, makes these materials very good candidates for electrodes in tunnel devices. However, all experimental studies agree[10, 11] to show that the TMR of manganites based devices decays rapidly with temperature and practically vanished much below room temperature, which in some manganites is below the Curie temperature (360K for $La_{2/3}Sr_{1/3}MnO_3$). The decay of the TMR with temperature has been ascribed to a reduction of the spin polarization at the electrode-barrier interface[11, 12, 13, 14].

Spin polarization experiments have shown that the magnetization of a free $La_{2/3}Sr_{1/3}MnO_3$ surface decreases much more rapidly with temperature than the spin polarization in bulk materials[7]. This degradation has been attributed to oxygen deficiency at the manganite surface, which splits the Mn e_g orbitals weakening the double exchange mechanism (DE)[15, 16, 17] for ferromagnetic (FM) order and favoring an antiferromagnetic (AF) arrangement of the Mn ions at the surface[18].

The manganite/insulator interface is different than the manganite surface. Recently, Garcia *et al.* [19] studied thermal decay of the spin polarization of $La_{2/3}Sr_{1/3}MnO_3$/insulator interface, and show that the magnetization of the interface can be as robust as that of the bulk. This result points out the difference between maganite/insulator interfaces and manganite surfaces and underscores the importance of the electronic carriers at the interfaces in order to obtain high temperature large TMR devices. Also Yamada *et al.*[20] have proved that by grading the doping profile at the interface, robust ferromagnetic order can be realized around room temperature. In this direction, Density Functional Theory based calculations[21] have shown that the magnetic character of the $La_{0.7}Sr_{0.3}MnO_3/SrTiO_3$ junction depends on the interface termination. The $La_{0.7}Sr/TiO_2$ interface is FM and metallic. However in the MnO_2/SrO interface the density of carriers is smaller and the DE mechanism is not strong enough to overcome the AF su-

perexchange interaction and the interface presents antiferromagnetic order. Also, recently Lin *et al.* [22] have studied the properties of double exchange superlattices, and predict a rich phase diagram, where the magnetic phases are correlated with the electronic charge distribution.

In the case of $La_{2/3}Ca_{1/3}MnO_3$ films on (001) $SrTiO_3$ substrates, NMR experiments have shown that an electronic phase separation into conducting and non conducting phases occurs close to the interface[13]. On the contrary, films grown on (110) substrates show no trends of electronic phase separarion[23]. Because the (001) films are fully strained whereas those grown on (110) are partially relaxed, the existence of electronic phase separation has been attribute to the strain. The strain induce a transition from a orbitally disordered ferromagnetic state to an orbitally ordered state associated with antiferromagnetic stacking of manganese oxides planes[24]. Epitaxial strain is also the responsible of the appearance of electronic phase separation in $La_{0.6}C_{0.4}MnO_3$ films grown on (100) $NdGaO_3$[25].

In this work we analyze theoretically the manganite/insulator interface. We use a microscopic model able to describe different exotic ground states that appear in bulk manganites at particular electron concentrations[26, 27, 28, 29].

We assume that the manganite has an ideal cubic perovskite structure , ABO_3. The Mn ions are located in the B sites and form a cubic lattice. The A sites of the perovskite crystal contain ions with average charge $(1-x)|e|$. The Mn ions have a core spin S=3/2, created by three electrons located in the deep energy t_{2g} levels. In addition there are $1-x$ electrons per unit cell, that hop between the e_g orbitals of the Mn ions. The carriers are coupled to the Mn's core spins through a very large Hund's coupling, in such a way that the motion of the carriers creates a long range ferromagnetic order. This mechanism for ferromagnetism is called double exchange interaction [15, 16, 17]. The DE competes with an AF superexchange coupling between the Mn core spins, and as result of this competition different exotic ground states emerge[26, 30, 31, 32].

We study a slab of manganite sandwiched into an insulator. We consider (001) manganite/insulator interfaces, where the average ionic charge changes from its bulk value to zero in a unit cubic lattice, see Fig.1. The long range Coulomb interaction is taken into account by the Hartree approximation. The main effect of the insulator is to confine the carriers to move in the manganite slab.

The main conclusion of our work is that electronic phase separation between a FM metallic phase and a spin and orbital ordered insulator phase is likely to occur at the manganite/insulator interface. This instability is favored by the reduction of carriers at the interface which weakens the FM coupling between the Mn ions, making more relevant the superexchange AF interaction. The ferromagnetic order at the interface can be recovered by inserting a small number of undoped $AMnO_3$ layers at the junction. Extra layers of $AMnO_3$ at the interface supply carriers to adjacent manganite slabs favoring a ferromagnetic interface.

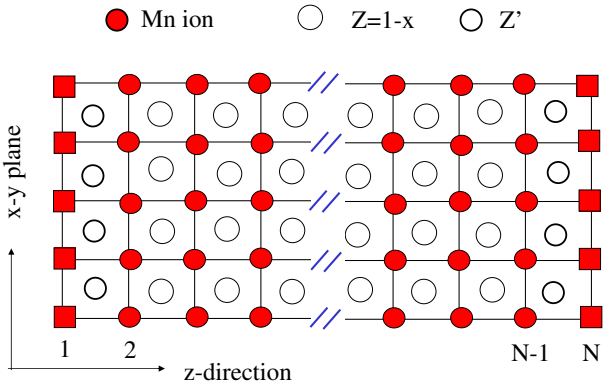

FIG. 1: (Color online) Schematic representation of the heterostructure studied in this paper. We choose the $x-y$ plane as the interface and z as the growth direction. The red circle denote the Mn ions. The green shaded and open circles represent ions of charge $Z=1-x$ and Z' respectively. The red squares show the sites where, because of the confinement by the insulator, the wavefunctions of the carriers has to be zero.

The rest of the paper is organized in the following way; In Section II we introduce the microscopic model and we discuss the more relevant electronic and magnetic phases that appear in bulk manganites. In Section III we show the electronic and magnetic phases that appear at the manganite/insulator interface as function of the strength of the long range Coulomb interaction and the superexchange AF coupling between the Mn ions. We study the case of a simple manganite/insulator interface and also we analyze how the properties of the interface are modified when a layer of undoped manganite is introduced at the interface. In Section IV we summarize our results.

II. MODEL

Heterostructure geometry. In the cubic perovskites the Mn ions are located at positions $\mathbf{R}_i = a(n_i, m_i, z_i)$ and form a cubic structure of lattice constant a. The positions A of the perovskite $AMnO_3$, $\mathbf{R}_i^A = a(n_i + 1/2, m_i + 1/2, z_i' + 1/2)$, are occupied, in the proportion $R_{1-x}D_x$, either by a rare ion ,R, or by a a divalent alkaline ion ,D. The divalent and trivalent atoms have a ionic charge +1 and 0 respectively, with relation to the Mn site. In our model we consider a (100) $AMnO_3$ slab containing N planes of MnO_2 intercalated by N-1 planes of AO. We consider periodic boundary conditions in the x and y directions. In the z-direction the positions of the Mn ions run from $z_i = 1$ to $z_i = N$, whereas the positions of

the counterions run from $z_i' = 0$ to $z_i' = N - 1$.

This slab is confined by a wide gap insulator,e.g. $TiSrO_3$. The insulator is described in our model by infinity potential barriers that confine the itinerant carriers to move in the manganite slab.

In order to simulate two symmetric manganite/insulator interface, we locate in the two outmost AO planes atoms with an ionic charge Z'. The Z'=0 case corresponds to a divalent atom and represents an interface with a deficit of electron charge. The Z'=1 case corresponds to a trivalent ion and in this situation there is an excess of electron carriers at the interface. In the central part of the slab we describe a manganite of formula $R_{1-x}D_xMnO_3$ by locating in the sites A of the crystal structure virtual ions of charge $Z|e| = (1-x)|e|$. The charge neutrality requires to get an electron concentration per Mn ion of [(N-3)(1-x)+2Z']/N.

With this geometry the insulator confines the carriers to move in the manganite region, and the long range Coulomb interaction forces the electronic charge to follow the spatial distribution of the charged ions.

Microscopic Hamiltonian. In the manganites the crystal field splits the Mn d levels into a fully occupied strongly localized t_{2g} triplet and a doublet of e_g symmetry. For manganites of composition $R_{1-x}D_xMnO_3$, there are $1-x$ electrons per Mn that hop between the e_g Mn states. The Coulomb interaction between electrons prevents double occupancy and aligns the spins of the d orbitals. The Hund's coupling between the spins of the carriers and each core spin is much larger than any other energy in the system, and each electron spin is forced to align locally with the core spin texture. Then the carriers can be treated as spinless particles and the hopping amplitude between two Mn ions is modulated by the spin reduction factor,

$$f_{12} = \cos\frac{\vartheta_1}{2}\cos\frac{\vartheta_2}{2} + e^{i(\phi_1-\phi_2)}\sin\frac{\vartheta_1}{2}\sin\frac{\vartheta_2}{2} \qquad (1)$$

where ϑ_i and ϕ_i are the polar and azimuthal angles Euler angles of the, assumed classical, Mn core spin $\mathbf{S}_i$. This is the so called DE model[15, 16, 17].

The microscopic Hamiltonian we study has the following terms,

$$H = H_{DE} + H_{AF} + H_{U'} + H_{Coul} \qquad (2)$$

The first term, H_{DE} describes the motion of the carriers,

$$H_{DE} = -\sum_{i,j,a,a'} f_{i,j}\, t^u_{a,a'}\, C^+_{i,a} C_{j,a'} \ , \qquad (3)$$

where $C^+_{i,a}$ creates an electron in the Mn ions located at site i in the e_g orbital a (a=1,2 with 1=$|x^2-y^2>$ and 2=$|3z^2-r^2>$). The hopping amplitude is finite for next neighbors Mn and depends both on the type of orbital involved and on the direction u between sites i and j ($t^{x(y)}_{1,1} = \pm\sqrt{3}t^{x(y)}_{1,2} = \pm\sqrt{3}t^{x(y)}_{2,1} = 3t^{x(y)}_{2,2} = t$)[32]. Along this work t is taken as the energy unit.

The second term describes the AF coupling between first neighbors Mn core spins,

$$H_{AF} = J_{AF} \sum_{<i,j>} \mathbf{S}_i \mathbf{S}_j \ , \qquad (4)$$

being J_{AF} the strength of the antiferromagnetic coupling between the Mn core spins.

In Eq.2, the term

$$H_{U'} = U' \sum_i \sum_{a\neq a'} n_{i,a} n_{i,a'} \ , \qquad (5)$$

with $n_{i,a} \equiv C^+_{i,a} C_{i,a}$, is a repulsive interaction between electrons in the same ion, but when they are in different orbitals.

Finally, the last term of Eq.2 describe the long-range Coulomb interaction between the charges in the system.

$$H_{Coul} = \frac{e^2}{\epsilon}\sum_{i\neq j} \left[\frac{1}{2}\frac{<n_i><n_j>}{|\mathbf{R}_i - \mathbf{R}_j|} + \frac{1}{2}\frac{Z_i Z_j}{|\mathbf{R}^A_i - \mathbf{R}^A_j|} - \frac{Z_j <n_i>}{|\mathbf{R}_i - \mathbf{R}^A_j|}\right] \ , \qquad (6)$$

here $<n_i> = \sum_a <C^+_{i,a} C_{i,a}>$ is the occupation number of the Mn ion locates at site $\mathbf{R}_i$, $Z_i e$ is the average charge of the ion locate at sites $\mathbf{R}^A_i$ and ϵ is the dielectric constant of the material.

Energy scales and mixing terms. In this model there are four energy scales, the hopping amplitude t, the AF coupling between Mn ions, the Hubbard term U' and the screening parameter, $\alpha = e^2/a\epsilon t$, which measures the strength of Coulomb interaction[22]. The manganites with a FM metallic ground state are characterized by a bandwidth of order 4-6eV and a background dielectric constant $\epsilon \sim 5-10$ implying a value of α in the range 0.7-2. The AF coupling is the smallest parameter, which according to some estimations, is $J_{AF} \sim 0.1t$[32, 33]. Even with this small value J_{AF} play a fundamental role in stabilizing interesting experimentally observed phases of manganites[27, 30, 32]. The Hubbard term U' has been included in the Hamiltonian for stabilizing, at moderate values of J_{AF}, the magnetic A phase at x=1. In the A phase, a Mn spin is ferromagnetically coupled with the Mn spins located in the same plane $(x-y)$, and antiferromagnetically with the Mn spins belonging to different planes. The value U'=2t, stabilizes the A phase at $x = 1$, and does not affect the phase diagram at other hole concentrations.

A relevant contribution to the Hamiltonian which has been not included in Eq.2, comes from the lattice deformation. In orbital ordered phases, it is possible to reduce considerable the energy by coupling the orbital order with the Jahn-Teller deformation of the oxygen octahedra surrounding the Mn ions. In large extent the lattice contribution of the ground state energies can be described by using effective values of J_{AF}[30], and therefore the value of the AF coupling that we use in our model

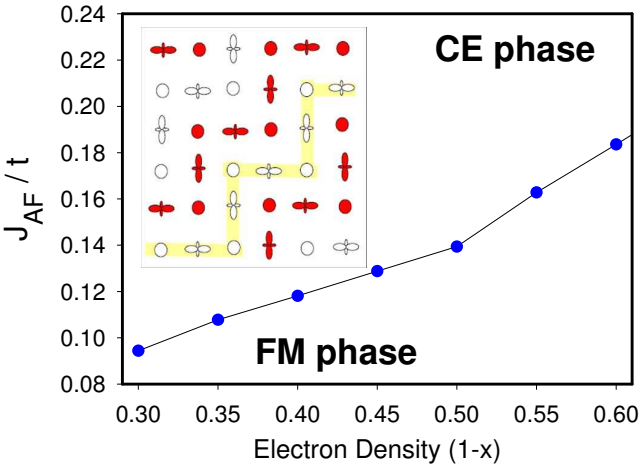

FIG. 2: (Color online) Bulk phase diagram $J_{AF} - (1-x)$ for x near x=1/2. In the inset it is represented the orbital and spin order of the CE phase at x=1/2. Elongated orbitals along the $x(y)$ directions represent $d_{3z^2-r^2}(d_{3y^2-r^2})$ orbitals. Circles represent $d_{x^2-y^2}$ orbitals. Red and white symbols indicate up and down Mn spins respectively. Shaded regions emphasize the CE zigzag chain. The line separating the FM phase from the CE phase is practically independent of U' and α for realistic values of these parameters ($U' < 4t$, and $\alpha < 2t$).

may be larger than the expected from magnetic neutron scattering experiments[33].

For a given value of the parameters U', α and J_{AF}, and a texture of core spins $\{\mathbf{S}_i\}$, we solve self-consistently the mean field version of Hamiltonian (2) and obtain the energy, the local charges $\{\rho_i\}$ and the orbital order $\{\tau_{xi}, \tau_{zi}\}$. The orbital order is characterized by the expectation value of the x and z components of the orbital pseudospin, $\tau_{xi} = C^+_{i1}C_{i2} + C^+_{i2}C_{i1}$ and $\tau_{zi} = C^+_{i1}C_{i1} - C^+_{i2}C_{i2}$, respectively.

A. Relevant bulk phases.

The ground state properties of manganites are determined by the competition between the energy scales: J_{AF}, U', t, α. In manganites, the energies involved in these interactions are comparable so very different states can have very similar energies. That is the reason why by slightly varying parameters such as carrier concentration, strain, disorder, or temperature, different ground states such as ferromagnetic metallic phases[34], AF Mott insulator[35], charge and orbital ordered stripe phases[36, 37, 38, 39], or ferromagnetic charge ordered phases[40] can be experimentally observed. We have checked that the Hamiltonian Eq.2 with the appropriated parameters describes the bulk ground states previously reported[26, 30, 32, 41].

At the manganite/insulator interface, the electron concentration falls from $1-x$ to zero in a couple of lattice parameters. In order to analyze the electronic reconstructions at the interface, it is convenient to study the bulk properties as function of the electron concentration. In Fig.2 we plot the $J_{AF} - (1-x)$ phase diagram near $x = 1/2$. Here we only consider the main two phases: the FM metallic phase and the CE phase. In the CE phase, the x-y layers are AF coupled while the magnetic structure within the planes is that of ferromagnetic zig-zag chains coupled antiferromagnetically[34]. The horizontal (x) and vertical (y) steps of the zig-zag chains contain three Mn ions. In the CE phase the charge is stacked in the z-direction whereas in the x-y planes it is ordered in a checkerboard form. Due to form of the e_g orbitals, the hopping amplitude between two Mn depends on the type of orbitals involved and on the direction of the vector linking the ions. In the CE phase, the system takes advantage of this effect, and creates an orbital ordering along the zig-zag chain, in such a way that the system opens a gap at the Fermi energy[27]. The orbital ordering is described by a uniform z-orbital pseudospin, $\tau_{z,i}$ and two finite Fourier components of the x-component of the pseudospin, $\hat{\tau_x}(\pi/2, \pi/2) = \hat{\tau_x}(-\pi/2, -\pi/2) \neq 0$. In the CE phase the manganites are band insulators and the gap is created by the orbital order. Note that electron charge modulation is only present for Jahn-Teller coupling different from zero. The cusp at x=1/2 in the line separating the FM phase from the CE phase indicates the existence of the electronic gap. Note in Fig.2 that the critical J_{AF} value for the FM to CE transition increases with the electron concentration. This is because the kinetic energy of the metallic FM phase increases with electron density, and it is necessary larger AF interaction for overcoming it.

In Fig.2 we have not consider the A phase or other more sophisticated phases[27, 32] that can appear when moving from half filling. These phases are very close in energy to the CE phase, they also represent orbital and spin ordered phases and filled only a small part of the phase diagram. Therefore for simplicity we ignore them and just consider the competition between the CE and the FM phase.

In Section III, we are going to consider the manganite/insulator interface modified by introducing an undoped manganite layer. In that case the density of electrons changes from the unity to zero at the interface. Experimentally[42], undoped manganites of small ionic radius, as $LaMnO_3$, are insulators and have an AF order type A. In the A phase, a Mn spin is ferromagnetically coupled with the Mn spins located in the same plane ($x-y$), and antiferrimagnetically with the Mn spins belonging to different planes. In Fig.3 we plot the $J_{AF} - (1-x)$ phase diagram near $x = 0$. By increasing the AF coupling the system undergoes a FM-AFM transition at a x-dependent critical value J^C_{AF}. For hole concentration greater than x=0.1, J^C_{AF} increases with the electron density, reflecting the increase of the kinetic en-

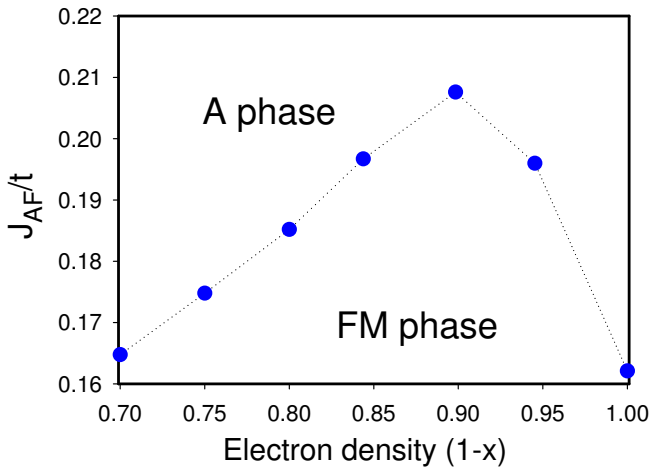

FIG. 3: (Color online) Bulk phase diagram $J_{AF} - (1-x)$ for x near x=0.

ergy. J_{AF}^{C} has a maximum near $x = 0.9$, and present a minimum for x=1. This minimum occurs because the A phase is an orbital ordered phase with a gap at the fermi energy. Near x=0, the A phase competes in energy with the E phase[29]. Be use a Hubbard term, $U' = 2t$, in order to privilege the A phase, and describe correctly the ground state of $LaMnO_3$. This value of U' practically unaffect the phase diagram of the manganites near half doping.

III. MANGANITE/INSULATOR INTERFACE. RESULTS

We have solved self-consistently the mean field version of Hamiltonian (2) for manganite/insulator interfaces, see Fig1, with different spin textures. We analyze two extreme cases; the Z'=0 case where there is a deficit of charge at the interface and the Z'=1 case where extra carriers are confined at the interface.

A. Z'=0. Defect of electron charge

In Fig.4 we plot the electronic charge on the Mn ions in a FM slab of $R_{0.7}D_{0.3}MnO_3$ containing 16 planes of MnO_3. In the case of zero Coulomb interaction (α=0) the electronic charge oscillates slightly around $< n_i >\sim$0.65 that is the average charge per electronic active Mn. These fluctuations are Friedel like oscillations and appear because of the confinement of the carriers to move into the slab. In the absence of Coulomb interaction the charge on Mn ions drops abruptly to zero in just one lattice spacing. When increasing the Coulomb interaction the electronic charge wants to screen the background of positive charge created by the counterions and approaches the bulk value

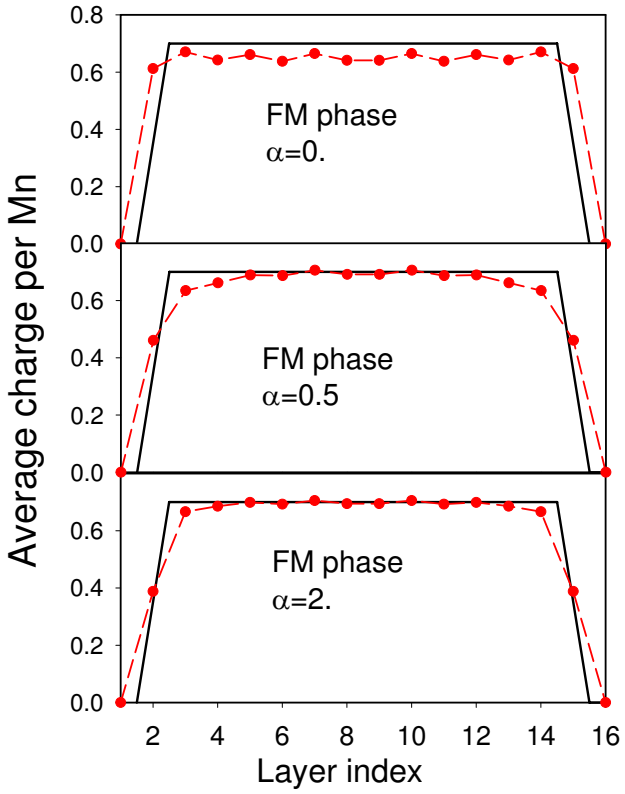

FIG. 4: (Color online) Electronic charge on the Mn ions, calculated in the FM phase, for different values of the Coulomb interaction α. The calculation is done in a slab formed by 16 layers of MnO_2. The continuous line represents the background of positive charge created by the ions located in the AO layers. The electron wavefunctions are forced to be zero at the first and last MnO_2 layers.

$< n_i >$=0.7 at the center of the slab. Also, at the interface, the electronic charge drops smoother from $< n_i >\sim$ 0.7 to $< n_i >$=0, as the Coulomb interaction parameter α increases. For moderate values of the Coulomb interaction, there is a MnO_2 slab at the manganite/insulator interface where the average electronic charge is close to $< n_i >$=0.5. Since near half doping the manganites can be unstable to form CE-type AF order, we also have studied interfaces where in one or two MnO_2 layers, the core spins of the Mn ions are CE ordered.

In Fig.5 we plot the average electronic charge on Mn ion in a slab of $R_{0.7}D_{0.3}MnO_3$ where the two pairs of electronic active MnO_2 layers closest to the interfaces are AF-CE ordered. In absence of Coulomb interactions, the electronic charge in the CE layers is pinned to a value closer to $< n_i >$=1/2. These plateaus in the charge density reflects the incompressibility of the electronic system at half doping in the CE phase, see Fig.2. As the Coulomb interaction increases the electron charge prefers to follow the profile defined by the counterions and the plateau in the electronic density profile becomes weaker. In any case, the existence of a region of incompressible

electronic density is evident in the charge density profile even for rather large Coulomb interaction.

The differences in energy between the FM phase and the phases containing AF-CE ordered MnO_2 layers depend on the Coulomb interaction, α, and the superexchange AF coupling, J_{AF}. In Fig.6 we plot the phase diagram α-J_{AF} for a system with a bulk hole concentration x=0.3. For a fix value of α, the number of CE layers in the slab near the interface increases as the AF coupling increases. For larger values of J_{AF} than those shown in Fig.6, all the Mn ions in the slab order in the AF-CE phase. An important point to note in Fig.6, is that the critical value of the AF coupling for the appearance of an AF-CE MnO_2 layer at the manganite/insulator interface is considerable smaller than the critical value for the occurrence of the x=1/2 AF-CE phase in bulk manganite. In bulk a value of J_{AF} larger than $0.14t$ is necessary for the occurrence of the CE phase at x=1/2, whereas at the interface values of J_{AF} smaller that $0.1t$ can induce phase separation between FM metallic phases and AF-CE insulating phase at the manganite/insulator interface. In Fig.6 we observe that the critical J_{AF} for the appearance of a CE MnO_2 layer decreases slightly with α. This is because as α increases the electron concentration in the last MnO_2 layer decreases, see Fig.4, and according with the phase diagram, Fig.2, the critical J_{AF} also decreases.

B. Z'=1. Excess of electronic charge.

The phase separation between CE and FM phases at the manganite /insulator interface that occurs in the Z'=0 case is due to the lack of electronic charge in the last MnO_2 planes. In the Z'=0 case the electronic charge per Mn in these planes is close to 0.5, and the system is unstable against CE magnetic order. An evident way to prevent the existence of phase separation is increasing the electron carrier at the interface. This can be done by inserting a layer of undoped manganite, $LaMnO_3$, at the interface[20]. We simulate this layer by locating trivalent ions, Z'=1, in the outmost AO layers and adding the corresponding extra electrons to the system.

In Fig.7, we plot the electronic charge on the Mn ions in a slab of $AMnO_3$, where the 13 central planes of AO contain counterions of average charge $(1-x)|e|$ and the two extremal AO planes contains trivalent ions of charge Z'=1. We assume that the Mn ions are ferromagnetically ordered. Fig.7(a) corresponds to the zero Coulomb interaction case, α=0. The electronic charge oscillates near the value of the average charge per electronic active Mn, $< n_i > \sim 0.79$. When the Coulomb interaction increases, Fig.7(b), the electronic charge wants to follow the background of positive charge created by the counterions. For large enough values of the Coulomb interaction (α=2), the electronic charge in the central layer of the slab gets its bulk value $< n_i > \sim 0.7$. The excess of charge is located at the interface, and the charge per Mn ion in the outmost MnO_2 layers is larger than the unity.

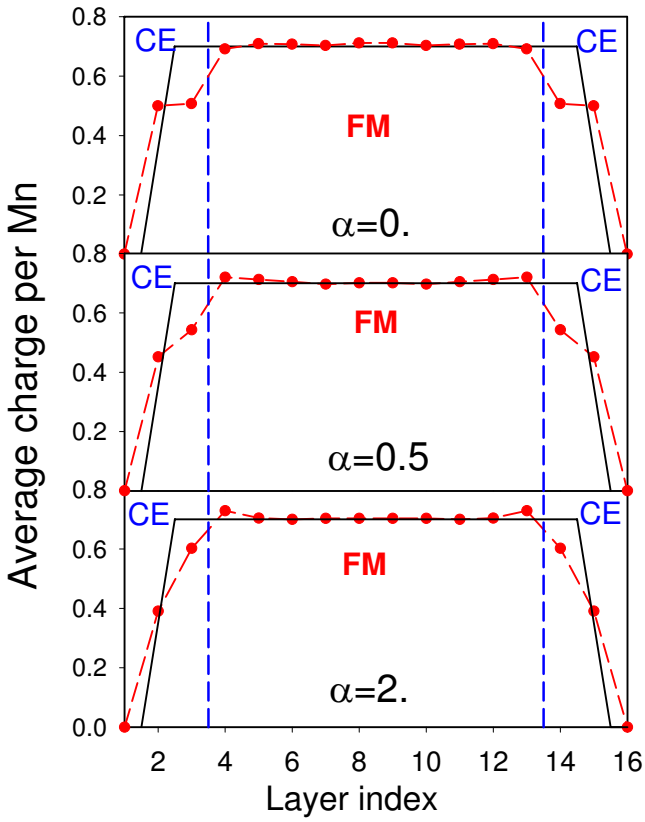

FIG. 5: (Color online) Electronic charge on the Mn ions for different values of the Coulomb interaction α. In this calculation the two first and two last electronic active MnO_2 layers have an antiferromagnetic order of type CE. The vertical dashed lines indicate the border between the FM region and the CE layers. The calculation is done in a slab formed by 16 layers of MnO_2. The continuum line represents the background of positive charge created by the ions located in the AO layers. The electron wavefunctions are forced to be zero at the first and last MnO_2 layers.

This excess of charge prevents the instability against CE magnetic order and phase separation. The insertion of a $LaMnO_3$ layer at the manganite/insulator interface increases the electron density at the junction , reinforces the DE mechanism and suppress AF instabilities at the interface.

In Fig.7 we can see that in the outmost layers the electron concentration is close to unity, and the system could be unstable to flip the spin of the MnO_2 layers close to the interface and form A-like AF structures. We have compared the energy of the FM state with the energy of a phase where the Mn core spins of the two extreme electronic active MnO_2 layers are antiparallel to the bulk FM polarization. In the inset of Fig.7 we plot the phase diagram $\alpha - J_{AF}$ for the slab described above. The main message of this results is that for realistic values of the AF coupling and Coulomb interaction, the system is FM.

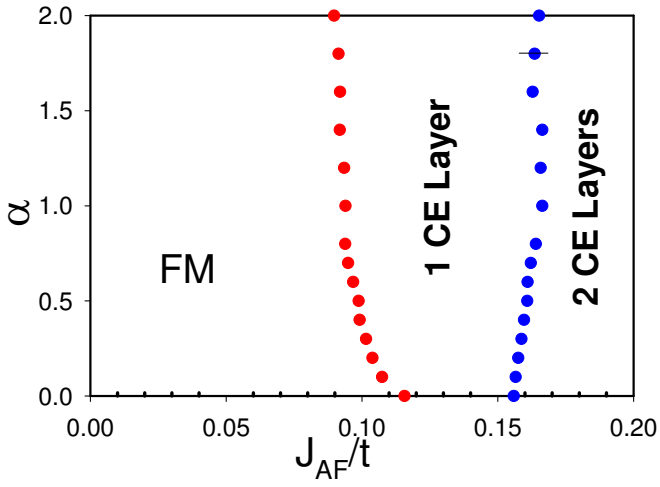

FIG. 6: (Color online) Phase diagram $J_{AF} - \alpha$ for a manganite/insulator interface. In bulk, the manganite has a hole concentration x=0.3. The error bar is an estimation of the numerical error in the calculations.

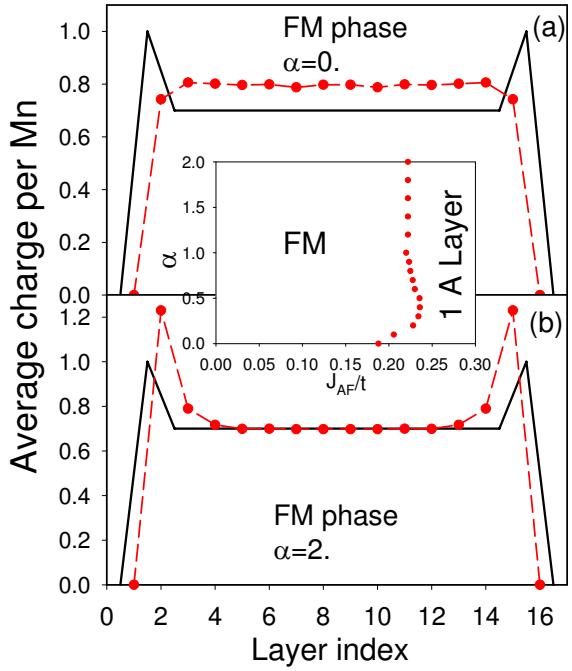

FIG. 7: (Color online)Electronic charge on the Mn ions, calculated in the FM phase, (a) for α=0 and (b) for α=2. The calculation is done in a slab formed by 16 layers of MnO_2. The continuous line represents the background of positive charge created by the ions located in the AO layers, Z'=1. The electron wavefunctions are forced to be zero at the first and last MnO_2 layers. The inset is the phase diagram α-J_{AF}. For realist values of the AF coupling, the core spins of all the electronic active Mn are ferromagnetically ordered.

IV. SUMMARY

We have studied the magnetic and electronic properties of an manganite/insulator interface. We analyze (001) interfaces, where the average ionic charge changes from its bulk value to zero in a unit cubic lattice. We model the manganites with a realistic microscopic model that describes adequately the different electric and magnetic phases experimentally observed in bulk. The long range Coulomb interaction is taken into account by the Hartree approximation. The main effect of the insulator is to confine the carriers to move in the manganite slab. We find that a electronic phase separation between a FM metallic phase and a spin and orbital ordered insulator phase is likely to occur at the manganite/insulator interface. This instability is favored by the reduction of carriers at the interface which weakens the FM coupling between the Mn ions, making more relevant the superexchange AF interaction. The insertion of a $LaMnO_3$ layer at the manganite/insulator interface introduces extra carriers at the junction which reinforce the DE mechanism and the FM long range order, suppressing AF instabilities at the interfaces.

V. ACKNOWLEDGMENTS

The author thanks J.Salafranca, J.Santamaria and I.C.Infante for helpful discussions. Financial support is acknowledged from Grant No MAT2006-03741. (Spain).

[1] J.S.Moodera and G.Mathon, J.Magn. Magn. Mater. **200**, 248 (2001).
[2] P. Grunberg, Physics Today **54** (2001).
[3] M. Julliere, Phys. Lett. **54A**, 225 (1975).
[4] J.C.Slonczewski, Phys. Rev. B **39**, 6995 (1989).
[5] L.Brey, C.Tejedor, and J.Fernández-Rossier, Appl.Phys..Lett. **85**, 1996 (2004).
[6] J.M.D.Coey and S.Sanvito, J. Phys, D **37**, 988 (2004).
[7] J.-H. Park, E. Vescovo, H.-J. Kim, C. Kwon, R. Ramesh, and T. Venkatesan, Phys. Rev. Lett. **81**, 1953 (1998).
[8] M. Viret, M. Drouet, J. Nassar, J.-P. Contour, C. Fermon, and A. Fert, Europhys. Lett. **39**, 545 (1997).
[9] M. Bowen, M. Bibes, A. Barthelemy, J.-P. Contour, A. Anane, Y. Lematre, and A. Fert, Appl.Phys.Lett. **82**, 233 (2003).
[10] Y. Lu, X. W. Li, G. Q. Gong, G. Xiao, A. Gupta, P. Lecoeur, J. Z. Sun, Y. Y. Wang, and V. P. Dravid, Phys. Rev. B **54**, R8357 (1996).
[11] M. Izumi, Y. Ogimoto, Y. Okimoto, T. Manako, P. Ahmet, K. Nakajima, T. Chikyow, M. Kawasaki, and Y. Tokura, Phys. Rev. B **64**, 064429 (2001).
[12] P. LeClair, H. J. M. Swagten, J. T. Kohlhepp, R. J. M. van de Veerdonk, and W. J. M. de Jonge, Phys. Rev. Lett. **84**, 2933 (2000).
[13] M. Bibes, L. Balcells, S. Valencia, J. Fontcuberta, M. Wojcik, E. Jedryka, and S. Nadolski, Phys. Rev. Lett. **87**, 067210 (2001).
[14] M. Bibes, S. Valencia, L. Balcells, B. Martínez, J. Fontcuberta, M. Wojcik, S. Nadolski, and E. Jedryka, Phys. Rev. B **66**, 134416 (2002).
[15] C.Zener, Phys. Rev. **82**, 403 (1952).
[16] P. Anderson and H.Hasewaga, Phys. Rev. **100**, 675 (1955).
[17] P.-G. de Gennes, Phys. Rev. **118**, 141 (1960).
[18] M. J. Calderón, L. Brey, and F. Guinea, Phys. Rev. B **60**, 6698 (1999).
[19] V. Garcia, M. Bibes, A. Barthelemy, M. Bowen, E. Jacquet, J.-P. Contour, and A. Fert, Phys. Rev. B **69**, 052403 (2004).
[20] H. Yamada, Y.Ogawa, Y. Ishii, H.Sato, M. Kawasaki, , H.Akoh, and Y. Tokura, Science **305**, 646 (2004).
[21] H.Zenia, G.A.Gehring, and W.M.Temmerman, cond-mat/0604343.
[22] C. Lin, S. Okamoto, and A. J. Millis, Phys. Rev. B **73**, 041104 (2006).
[23] J.Fontcuberta, I. Infante, V. Laukhin, F. Sanchez, M. Wojcik, and E. J. E, J. Appl. Phys. **99**, 08A701 (2006).
[24] J. Klein, J. B. Philipp, G. Carbone, A. Vigliante, L. Alff, and R. Gross, Phys. Rev. B **66**, 052414 (2002).
[25] D. Sanchez, L. Hueso, L. Granja, P. Levy, and N. Mathur, cond-mat/0605187.
[26] L. Brey, Phys.Rev.Lett. **92**, 127202 (2004).
[27] L. Brey and P. B. Littlewood, Phys. Rev. Lett. **95**, 117205 (2005).
[28] L. Brey, Phys. Rev. B **71**, 174426 (2005).
[29] J. Salafranca and L. Brey, Phys. Rev. B **73**, 024422 (2006).
[30] J. van den Brink, G.Khaliullin, and D.Khomskii, Phys. Rev. Lett. **83**, 5118 (1999).
[31] D.Arovas, G.Gómez-Santos, and F.Guinea, Phys. Rev. B **59**, 13569 (1999).
[32] E. Dagotto, *Nanoscale Phase Separation and Colossal Magnetoresistance* (Springer-Verlag, Berlin, 2002).
[33] T. G. Perring, G. Aeppli, Y. Moritomo, and Y. Tokura, Phys. Rev. Lett. **78**, 3197 (1997).
[34] E.O.Wollan and W. Koehler, Phys. Rev. **100**, 545 (1955).
[35] J.Kanamori, J. Appl. Phys. (Suppl.) **31**, 14S (1960).
[36] C.H.Chen and S.-W. Cheong, Phys. Rev. Lett. **76**, 4042 (1996).
[37] C.H.Chen, S.-W. Cheong, and H.Y.Hwang, J. Appl. Phys. **81**, 4326 (1997).
[38] S.Mori, C.H.Chen, and S.-W. Cheong, Nature **392**, 473 (1998).
[39] C.H.Chen, C.H.Mori, and S.-W. Cheong, J. Phys. IV France **9**, Pro10 (1999).
[40] J.C.Loudon, N.D.Mathur, and P. Midgley, Nature **420**, 797 (2002).
[41] I.Solovyev and K.Terakura, Phys. Rev. Lett. **83**, 2825 (1999).
[42] K.Kimura, S.Ishihara, H.Shintani, T.Arima, K.T.Takahashi, K.Ishizaka, and Y.Tokura, Phys.Rev.B **68**, 060403 (2003).